ORIGINAL PAPER

Cory A. Christensen · Edward J. King
John R. Jordan · Gary N. Drews

Megagametogenesis in *Arabidopsis* wild type and the *Gf* mutant

Abstract The female gametophyte is an essential structure for angiosperm reproduction that mediates a host of reproductive functions and, following fertilization, gives rise to most of the seed. Here, we describe a rapid method to analyze *Arabidopsis* female gametophyte structure using confocal laser scanning microscopy (CLSM). We present a comprehensive description of megagametogenesis in wild-type *Arabidopsis*. Based on our observations, we divided *Arabidopsis* megagametogenesis into eight morphologically distinct stages. We show that synergid cell degeneration is triggered by pollination, that dramatic nuclear migrations take place during the four-nucleate stage, and that megagametogenesis within a pistil is fairly synchronous. Finally, we present a phenotypic analysis of the previously reported *Gf* mutant (Redei 1965) and show that it affects an early step of megagametogenesis.

Key words *Arabidopsis* · Confocal laser scanning microscopy · Female gametophyte · *Gf* mutant · Megagametogenesis · Plant reproduction

Introduction

The female gametophyte is an essential structure for sexual reproduction in angiosperms. Following pollination, the female gametophyte participates in directing pollen tube growth toward the ovule (Hulskamp et al. 1995). Fertilization takes place in the female gametophyte and is likely to be mediated by a host of female gametophyte-encoded products (van Went and Willemse 1984; Russell 1993). Upon fertilization, female gametophyte-expressed genes are involved in inducing seed development (Kermicle 1969; Kobayashi and Tsunewaki 1980; Tsunewaki and Mukai 1990; Ohad et al. 1996). During

C.A. Christensen · E.J. King · J.R. Jordan · G.N. Drews (✉)
Department of Biology, University of Utah, Salt Lake City,
UT 84112, USA
Tel. +1–801–585–6203; Fax +1–801–581–4668;
e-mail drews@bioscience.utah.edu

seed development, the female gametophyte's egg and central cells give rise to the seed's embryo and endosperm, respectively. The female gametophyte is also important for some forms of asexual reproduction, as in gametophytic apomixis for example (Nogler 1984; Koltunow 1993).

The female gametophyte has a variety of forms. The most common form, exhibited by 70% of the species examined, is monosporic-type megasporogenesis combined with *Polygonum*-type megagametogenesis (Maheshwari 1950; Willemse and van Went 1984; Reiser and Fischer 1993). During monosporic-type megasporogenesis, a diploid megaspore mother cell undergoes meiosis to produce four haploid megaspores. One of the megaspores survives and the other three degenerate. During *Polygonum*-type megagametogenesis, the functional megaspore undergoes three rounds of mitosis, producing an eight-nucleate cell. Nuclear migration and cellularization result in the seven-celled embryo sac depicted in Figs. 1A and 1B.

We have been using *Arabidopsis* to study *Polygonum*-type megagametogenesis. *Arabidopsis* megagametogenesis has been examined by light microscopy of paraffin-sectioned material (Misra 1962; Poliakova 1964) or of cleared ovules (Webb and Gunning 1994; Schneitz et al. 1995). We recently isolated a battery of mutants with defects in megagametogenesis or female gametophyte function (C. A Christensen, S. Subramanian, and G. N. Drews, unpublished). To facilitate the analysis of a large number of megagametogenesis mutants, we developed a rapid (1 day) procedure to analyze *Arabidopsis* megagametogenesis using confocal laser scanning microscopy (CLSM). CLSM is particularly well suited for the rapid analysis of female gametophyte development because specimen preparation does not require time-consuming physical sectioning and is substantially faster than the tissue clearing and staining procedures used with interference contrast microscopy. CLSM provides thin optical sections characterized by excellent resolution, high contrast, and near absence of out-of-focus information. Furthermore, CLSM serial optical sections can be assembled
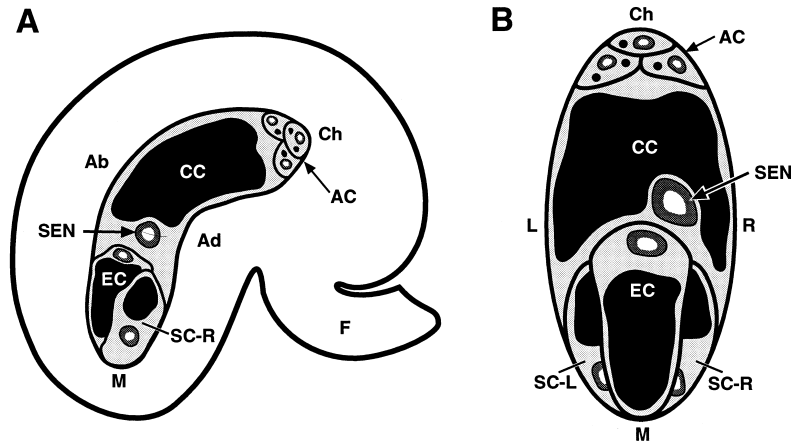
A

B

Fig. 1A, B Depiction of a seven-celled *Arabidopsis* female gametophyte. **A** Longitudinal view; **B** view from the abaxial direction. Depicted are cytoplasm (*light gray areas*), vacuoles (*black areas*), nuclei (*dark gray areas*), and nucleoli (*white areas* within the nuclei). The female gametophyte in **A** is oriented with its adaxial surface (adjacent to the funiculus; *Ad*) to the right, its abaxial surface (*Ab*) to the left, its micropylar pole (*M*) down, and its chalazal pole (*Ch*) up. The female gametophyte in **B** is oriented with its right surface (*R*) to the right, its left surface (*L*) to the left, its micropylar pole (*M*) down, and its chalazal pole (*Ch*) up. *AC* Antipodal cell, *CC* central cell, *EC* egg cell, *F* funiculus, *SC-L* "left" synergid cell, *SC-R* "right" synergid cell, *SEN* secondary endosperm nucleus

into digital volume sets that may be reoriented and/or resectioned to provide perspectives on the specimen that were not available in the specimen's original orientation (e.g., the data in Fig. 3).

In this paper we describe a rapid procedure to analyze *Arabidopsis* female gametophyte development using CLSM. We used this CLSM procedure to extend previous observations of *Arabidopsis* megagametogenesis (Misra 1962; Poliakova 1964; Webb and Gunning 1994; Schneitz et al. 1995). New observations allowed us to divide *Arabidopsis* megagametogenesis into eight morphologically distinct stages. We also used our CLSM procedure to analyze megagametogenesis in the previously-reported *Gf* mutant (Redei 1965). We show that the *Gf* mutation affects an early step of megagametogenesis.

Materials and methods

Plant material and growth conditions

Seeds were sown in Sunshine Mix #3 (Sun Gro Horticulture, Bellevue, Wash.). Plants were grown at 22°C and 50% relative humidity under eight fluorescent lamps (Sylvania cool white) in an EGC growth chamber. In each photoperiod, plants were given 18 h of illumination. Plants were watered three times per week. The *Gf* mutant was produced by X-ray irradiation in a Columbia background (Redei 1965). Because of the presence of additional mutations, the *Gf* mutant was backcrossed two generations before morphological analysis.

Confocal laser scanning microscopy

Pistils were dissected by first removing the sepals, petals and stamens from isolated flowers. Cuts were then made on both sides of the pistil replum using a 30.5-gauge syringe to expose the ovules to fixative. Pistils were fixed in a solution of 4% glutaraldehyde and 12.5 mM cocadylate (pH 6.9) for 2 h at room temperature. The initial 30 min of fixation was performed under a house vacuum (~200 torr). Following fixation, the tissue was dehydrated in a graded ethanol series (20% steps for 10 min each). Following dehydration, the tissue was cleared in a 2:1 mixture of benzyl benzoate:benzyl alcohol. The pistils were mounted in immersion oil (Scientific products high viscosity) and sealed under coverslips with fingernail polish.

A Bio-Rad MRC 600 laser scanning confocal system equipped with a Kr/Ar laser and mounted on a Nikon Optiphot was used to examine the female gametophytes within the pistils. The 568 nm laser line and YHS filter set were used to illuminate the siliques. Optical sections of 1.5 μm were collected with a Nikon Plan apo ×60 objective. Images were collected using Comos version 7.0a software (Bio-Rad).

NIH image version 1.58 software and Confocal Assistant version 3.08 software (copyright Todd Clarke Brelje) was used for subsequent image analysis. Voxblast version 1.2 software (Vay Tek) was used to perform three-dimensional reconstruction, three-dimensional measurements, and analysis. Figures were prepared using Canvas version 3.1 software (Deneba) and Photoshop version 3.0 software (Adobe). Prints were made with a Kodak 3600 dye sublimation printer.

With the CLSM procedure, cytoplasm, nucleoplasm and nucleoli exhibit autofluorescence when illuminated by the 488 nm or 568 nm laser lines. Fluorescence from cytoplasm and nucleoplasm is moderate and fluorescence from nucleoli is extremely bright. Fluorescence from cytoplasm and from nucleoplasm is approximately equal, but these two cellular compartments can be distinguished because nucleoplasm has a smoother texture (e.g., the central cell and egg cell nuclei in Fig. 7A). Nucleoli are distinguished by their extremely bright autofluorescence (all figures). Vacuoles are distinguished by having no fluorescence (all figures). Cell boundaries are distinguished by a dark line between two cells (e.g., the inner integument cells and the one-nucleate embryo sac in Fig. 2B, and the antipodal cells in Fig. 6A), by slight differences in cytoplasmic fluorescence between two adjacent cells (e.g., the synergid cells in Fig. 4C, D), or by vacuolar appression of cytoplasm (e.g., the outer integument cells in Fig. 2B, C and the synergid cells in Fig. 4C, D).

Flower development stages 12a, 12b, and 12c

For CLSM analysis, pistils were collected from flowers at specific stages of flower development (Smyth et al. 1990). As shown in Ta-
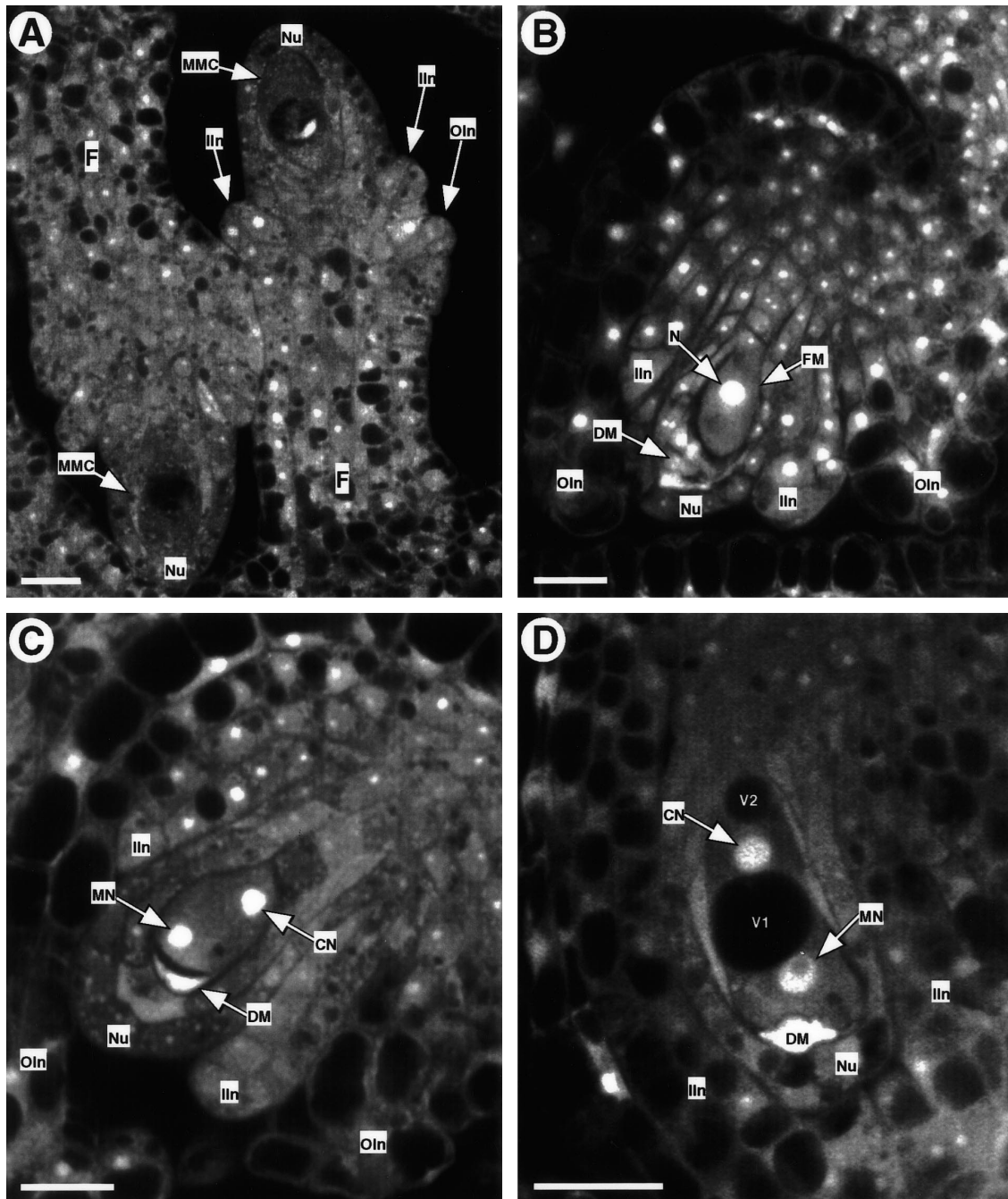
Fig. 2A–D Stages FG0–FG3 of *Arabidopsis* female gametophyte development. **A** Confocal laser scanning microscopy (CLSM) image of a female gametophyte at stage FG0. This panel shows the megaspore mother cell (*MMC*) surrounded by, and in direct contact with, the nucellar epidermis (*Nu*). At this stage, the outer (*OIn*) and inner (*IIn*) integuments have just initiated. This image consists of a single 1.5 μm optical section. **B** CLSM image of a developing female gametophyte at stage FG1. The developing female gametophyte [functional megaspore (FM)] is uninucleate (*N*) and teardrop-shaped. Degenerating megaspores (*DM*) are shown. The outer (*OIn*) and inner (*IIn*) integuments do not completely enclose the nucellus (*Nu*). This image consists of five 1.5 μm optical sections. **C** CLSM image of a developing female gametophyte at stage FG2. The developing female gametophyte consists of two nuclei with one nucleus (*MN*) toward the micropylar pole and the other nucleus (*CN*) toward the chalazal pole. The nucellus (*Nu*) is enclosed by the outer (*OIn*) but not by the inner integuments (*IIn*). This image is a projection of two 1.5 μm optical sections. **D** CLSM image of a developing female gametophyte at stage FG3. The developing female gametophyte consists of two nuclei (*CN* and *MN*) separated by a large central vacuole (*V1*). An FG3 female gametophyte also contains a smaller vacuole (*V2*) at its chalazal pole. At this and all subsequent stages the nucellus (*Nu*) is completely enclosed by the inner integuments (*IIn*). This image is a projection of two 1.5 μm optical sections. In all panels except **A**, the female gametophytes are oriented with the micropylar pole down and the chalazal pole up. *F* Funiculus. *Bars*=10 μm
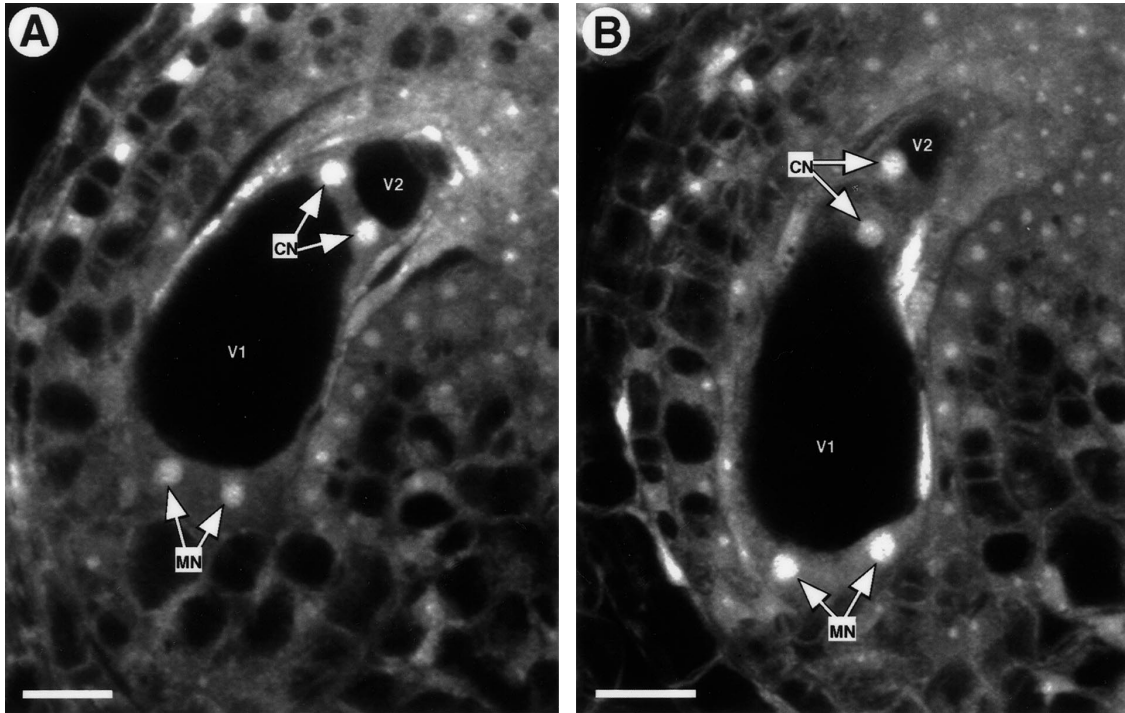
Fig. 3A, B Stage FG4 of *Arabidopsis* female gametophyte development. The developing female gametophyte consists of four nuclei. A large central vacuole (*V1*) separates a pair of chalazal nuclei (*CN*) from a pair of micropylar nuclei (*MN*). An FG4 female gametophyte also contains a smaller vacuole (*V2*) at its chalazal pole. **A** CLSM image of a developing female gametophyte at early stage FG4. The line between the two chalazal nuclei (*CN*) lies orthogonal to the chalazal-micropylar axis. This image is a projection of three 1.5 μm digital resections of the original volume data set. **B** CLSM image of a developing female gametophyte at late stage FG4. The line between the two chalazal nuclei (*CN*) lies parallel to the chalazal-micropylar axis. This image is a projection of four 1.5 μm digital resections of the original volume data set. In both panels, the female gametophytes are oriented with the adaxial surface to the right, the abaxial surface to the left, the micropylar pole down, and the chalazal pole up. For both panels, the raw two-dimensional data has been rendered into a volume using Voxblast software. The volume was then reoriented and resectioned to achieve the optimal view of the data. *Bars*=10 μm

ble 3, most female gametophyte development in *Arabidopsis* occurs during flower development stage 12. We therefore defined three substages that we refer to as 12a, 12b, and 12c. During stage 12a the petals are level with the long stamens. The petals are translucent and the anthers are green. During stage 12b the petals are longer than the stamens but are shorter than the sepals. The petals are milky-white (somewhat translucent) and the anthers are yellow-green. During stage 12c, the petals are equal to or longer than the sepals. Anthesis has not occurred. The petals are white and the anthers are yellow.

Assignment of a female gametophyte stage to a pistil

In most cases, a single female gametophyte stage predominates (≥75%) within a pistil. Under these circumstances, we assign one female gametophyte stage to a pistil. For example, pistils 1, 3, and 5 in Table 4 would be assigned stages FG0, FG1, and FG3, respec-

tively. In some cases, a single stage does not predominate because the pistil is at a transition between two stages. Under this circumstance, we assign the pistil the two stages that together constitute ≥75% of the female gametophytes. For example, pistils 2 and 10 in Table 4 would be assigned stages FG0/1 and FG5/6, respectively.

The imperfect synchrony of female gametophyte development was used to define female gametophytes at early and late stage FG4. We defined early stage FG4 female gametophytes as those found in pistils containing predominantly earlier stages (e.g., pistil number 5 in Table 4). By contrast, we defined late stage FG4 female gametophytes as those found in pistils containing predominantly later stages (e.g., pistil number 8 in Table 4).

Transmission electron microscopy

Pistils were cut into 1 mm segments and fixed overnight in a solution of 4% glutaraldehyde in 12.5 mM sodium cacodylate buffer (pH 6.9). The tissue segments were then washed in buffer, postfixed for 4 h in 1% aqueous osmium tetroxide, washed in distilled water, and postfixed for 1 h in 1% aqueous uranyl acetate. All solutions were kept at 4°C. The tissue was then dehydrated at room temperature in a graded ethanol series (20% steps for 20 min each), transferred into propylene oxide through intermediate stages of 1:2, 1:1, and 2:1 mixtures of propylene oxide:ethanol, and infiltrated and embedded in Embed 812 (Electron Microscopy Sciences). Thin sections (90 nm) were stained with 2% aqueous uranyl acetate and with Reynold's lead citrate, and examined in a Hitachi H-7100 electron microscope. Photographic images were recorded on Kodak 4489 electron microscope film.

Results

CLSM analysis

We developed a procedure to prepare *Arabidopsis* ovules for CLSM analysis (see Materials and methods). This

Table 1 Stages of *Arabidopsis* female gametophyte development

Stage	Female gametophyte morphology
FG1	One-nucleate female gametophyte. Teardrop shaped with the micropylar end being broader. Three degenerating megaspores are present.
FG2	Two-nucleate female gametophyte. Several small (<5 μm) vacuoles are present. During late stage FG2, the vacuoles begin to coalesce in the center. Degenerate megaspores are present.
FG3	Two-nucleate female gametophyte with a central vacuole. The two nuclei are located near the chalazal and micropylar poles. A large central vacuole is present between the nuclei and a second, smaller vacuole is usually present at the chalazal pole. Degenerate megaspores are present.
FG4	Four-nucleate female gametophyte. Two nuclei at each pole. The two pairs of nuclei are separated by a large central vacuole. A second, smaller vacuole is usually present at the chalazal pole. During early stage FG4, the chalazal nuclei lie along a line that is orthogonal to the chalazal-micropylar axis. During late stage FG4, the chalazal nuclei lie along a line that is parallel to the chalazal-micropylar axis.
FG5	Eight-nucleate/seven-celled female gametophyte with unfused polar nuclei. Initially, four nuclei at each pole. Cellularization begins immediately following mitosis and is completed by mid-stage FG5. During cellularization, one nucleus from each pole (polar nuclei) migrates toward the center.
FG6	Seven-celled female gametophyte with polar nuclei fused. During this stage, the three antipodal cells are in the process of degenerating.
FG7	Four-celled female gametophyte. The antipodal cells have degenerated. The female gametophyte is comprised of the egg cell, the central cell, and two synergid cells.
FG8	Three-celled female gametophyte. One of the synergid cells degenerates. The female gametophyte consists of the egg cell, the central cell, and one persistent synergid cell.

Table 2 Female gametophyte dimensions during development in L-*er*

Stage	Number analyzed	Length (μm)		Width (μm)	
		Mean	Range	Mean	Range
FG1 (One-nucleate)	10	13.19	12.01–15.99	6.72	5.67–7.91
FG2 (Early two-nucleate)	10	18.31	16.21–20.07	6.79	6.29–7.39
FG3 (Late two-nucleate)	10	25.89	20.53–29.43	10.04	6.87–12.64
FG4 (Four-nucleate)	10	52.70	32.93–66.00	18.51	15.75–21.36
FG5 (Eight-nucleate)	12	94.23	90.06–97.81	19.75	18.25–24.06
FG6 (Seven-celled)	6	98.77	94.67–104.00	23.60	23.08–24.01
FG7 (Four-celled)	4	95.00	94.74–95.79	23.71	22.99–24.01
FG8 (Three-celled)	2	104.77	104.23–105.32	25.35	24.99–25.71

procedure is extremely rapid (4 h) for two reasons. First, ovule dissection is not required. In this procedure, whole-mount pistils are fixed and mounted for CLSM analysis. Second, tissue is not stained. Rather, developing ovules exhibit autofluorescence. Fluorescence from nucleoli is extremely bright, and that from cytoplasm and nucleoplasm is moderate. By contrast, vacuoles do not autofluoresce. Nucleolar fluorescence makes female gametophyte nuclei distinct because, in *Arabidopsis* and many other species, embryo sac nuclei contain single nucleoli which are much larger than the nucleoli of the surrounding ovule cells (Willemse and van Went 1984; Mansfield et al. 1991). With this procedure, we can distinguish cytoplasm, nuclei, nucleoli, vacuoles, and cell boundaries (see Materials and methods). Because of the rapidity of this procedure and of CLSM analysis, we were able to observe over 1000 developing embryo sacs in our analysis of wild-type female gametophyte development.

Megagametogenesis in *Arabidopsis* wild type

We used our CLSM procedure to analyze wild-type megagametogenesis in the *Arabidopsis* ecotypes Landsberg *erecta* (L-*er*), Columbia, and Wassilewskija. We found no differences in megagametogenesis among these three ecotypes. To provide a framework for future genetic and molecular analysis, we divided *Arabidopsis* megagametogenesis into eight stages. Table 1 summarizes these eight female gametophyte stages. Table 2 gives the female gametophyte dimensions at each developmental stage in the L-*er* ecotype. Table 3 lists the flower and ovule developmental stages within which the female gametophyte stages occur.

Megasporogenesis (stage FG0)

Stage FG0 encompasses all of megasporogenesis. We found that the archesporial cell functions directly as the megaspore mother cell (Webb and Gunning 1990; Schn-

Table 3 Flower development and ovule stages during which the female gametophyte stages occur

Female gametophyte stage	Flower development stage[a]	Ovule development stage[b]
FG0 (Megasporogenesis)	11	2
FG1 (One-nucleate)	12a	3-I
FG2 (Early two-nucleate)	12b	3-II
FG3 (Late two-nucleate)	12b–12c	3-III
FG4 (Four-nucleate)	12b–12c	3-IV
FG5 (Eight-nucleate)	12b–13	3-V
FG6 (Seven-celled)	12c–14	3-VI
FG7 (Four-celled)	13–14	3-VI
FG8 (Three-celled)	14	–

[a] Flower development stages from Smyth et al. (1990); See Materials and methods for definitions of flower development stages 12a, 12b, and 12c

[b] Ovule development stages from Schneitz et al. (1995)

eitz et al. 1995) and that the megaspore mother cell is in direct contact with the nucellar epidermis (Fig. 2A). This indicates that the *Arabidopsis* ovule is tenuinucellate (Maheshwari 1950; Bouman 1984; Webb and Gunning 1990; Schneitz et al. 1995). Fig. 2A shows that the *Arabidopsis* nucellus is of the type that is elongated and in which the integuments arise near its base (Maheshwari 1950).

Fig. 2A shows the megaspore mother cell prior to meiosis. It is a relatively large cell (~17 μm) with a cytoplasm containing one or more vacuoles (data not shown). The diploid megaspore mother cell undergoes meiosis to form a tetrad of haploid megaspores. We generally observed T-shaped tetrads (Maheshwari 1950; Bouman 1984; Webb and Gunning 1990; Schneitz et al. 1995). We also observed linear tetrads (Misra 1962), but at a frequency far less than that of the T-shaped tetrads (Schneitz et al. 1995).

Shortly after meiosis, three of the megaspores degenerate, and one megaspore expands and gives rise to the female gametophyte. The degenerating megaspores were readily identified because they autofluoresced with elevated intensity when compared with the surviving megaspore and the surrounding ovule cells (Fig. 1C, D). The autofluorescence was perhaps due to the accumulation of callose in the walls of these cells (Webb and Gunning 1990). We found that it was the chalazal-most megaspore that survived (Fig. 1B) (Webb and Gunning 1990; Modrusan et al. 1994; Schneitz et al. 1995) and we found this to be the case in all of over 500 ovules examined; thus, there appears to be no exception to this rule. Survival of the chalazal-most megaspore is the usual condition in *Polygonum*-type female gametophyte development (Maheshwari 1950; Willemse and vanWent 1984; Haig 1990; Reiser and Fischer 1993).

One-nucleate stage (stage FG1)

Stage FG1, shown in Fig. 2B, is defined as the uninucleate female gametophyte stage. This stage occurs late during megasporogenesis, when the functional megaspore is expanded and the other three megaspores are undergoing degeneration. During stage FG1, the developing female gametophyte adopts a teardrop shape, with the micropylar end being the more expanded (Fig. 2B) (Webb and Gunning 1990). As stage FG1 progresses, the three degenerate megaspores become crushed at the micropylar end between the megaspore and the nucellar epidermis (Fig. 2B). Late in stage FG1, several small (<1 μm) vacuoles are observed (data not shown). At stage FG1, the ovule's inner integument is approximately one-half the length of the nucellus, and the outer integument surrounds the inner integument but does not completely enclose the nucellus. This is in contrast to Schneitz et al. (1995) who reported that the outer integument completely surrounds the nucellus at this stage.

Early two-nucleate stage (stage FG2)

Stage FG2 is shown in Fig. 2C. Stage FG2 begins as the functional megaspore undergoes mitosis, giving rise to a two-nucleate female gametophyte. Throughout stage FG2, several small vacuoles are present at various positions within the developing embryo sac, but toward the end of this stage, these vacuoles appear to coalesce in the center (data not shown). The developing female gametophyte continues to expand during this stage (Table 2).

Fig. 4A–D Stages FG5 and FG6 of *Arabidopsis* female gametophyte development. **A** CLSM image of a developing female gametophyte at early stage FG5. A large central cell vacuole (*CV*) separates two sets of nuclei. At the chalazal pole are three antipodal nuclei (*AN*) and one polar nucleus (*CPN*), and at the micropylar pole are two synergid nuclei (*SN*), one egg nucleus (*EN*), and one polar nucleus (*MPN*). This image is a projection of four 1.5 μm optical sections. **B** CLSM image of a developing female gametophyte at mid stage FG5. A large central cell vacuole (*CV*) separates two sets of cells. At the chalazal pole are three antipodal nuclei (*A1N*, *A2N*, and *A3N*), and at the micropylar pole are two synergid nuclei ("left" *SLN* and "right" *SRN*) and one egg nucleus (*EN*). The chalazal polar nucleus (*CPN*) and the micropylar polar nucleus (*MPN*) have migrated toward each other along the adaxial surface. This image is a projection of the four 1.5 μm optical sections shown in Fig. 5. *A1N*, *A2N*, *A3N*, *SLN*, and *SRN* correspond to the nuclei of the same names in Fig. 5. **C** CLSM image of a developing female gametophyte at late stage FG5. Polar nuclei migration is complete and the female gametophyte cells are fully cellularized. The two polar nuclei (*PN*) lie in close proximity to each other and to the egg cell nucleus (*EN*). The line between the polar nuclei (*PN*) is approximately perpendicular to the chalazal-micropylar axis. The "left" synergid cell (nucleus, *SLN* and vacuole, *SLV*) and the "right" synergid cell (nucleus, *SRN* and vacuole, *SRV*) lie side-by-side. This image is a projection of six 1.5 μm optical sections. **D** CLSM image of a developing female gametophyte at stage FG6. The polar nuclei have fused, yielding the secondary endosperm nucleus (SEN). This image is a projection of nine 1.5 μm optical sections. In all panels, the female gametophyte is oriented with the micropylar pole down and the chalazal pole up. The female gametophyte in **A** is oriented at an oblique angle. The female gametophyte in **B** is oriented with the adaxial surface to the right and the abaxial surface to the left. The female gametophytes in **C** and **D** are viewed from the abaxial surface such that the right surface is to the right and the left surface is to the left (defined in Fig. 1). *Bars*=10 μm
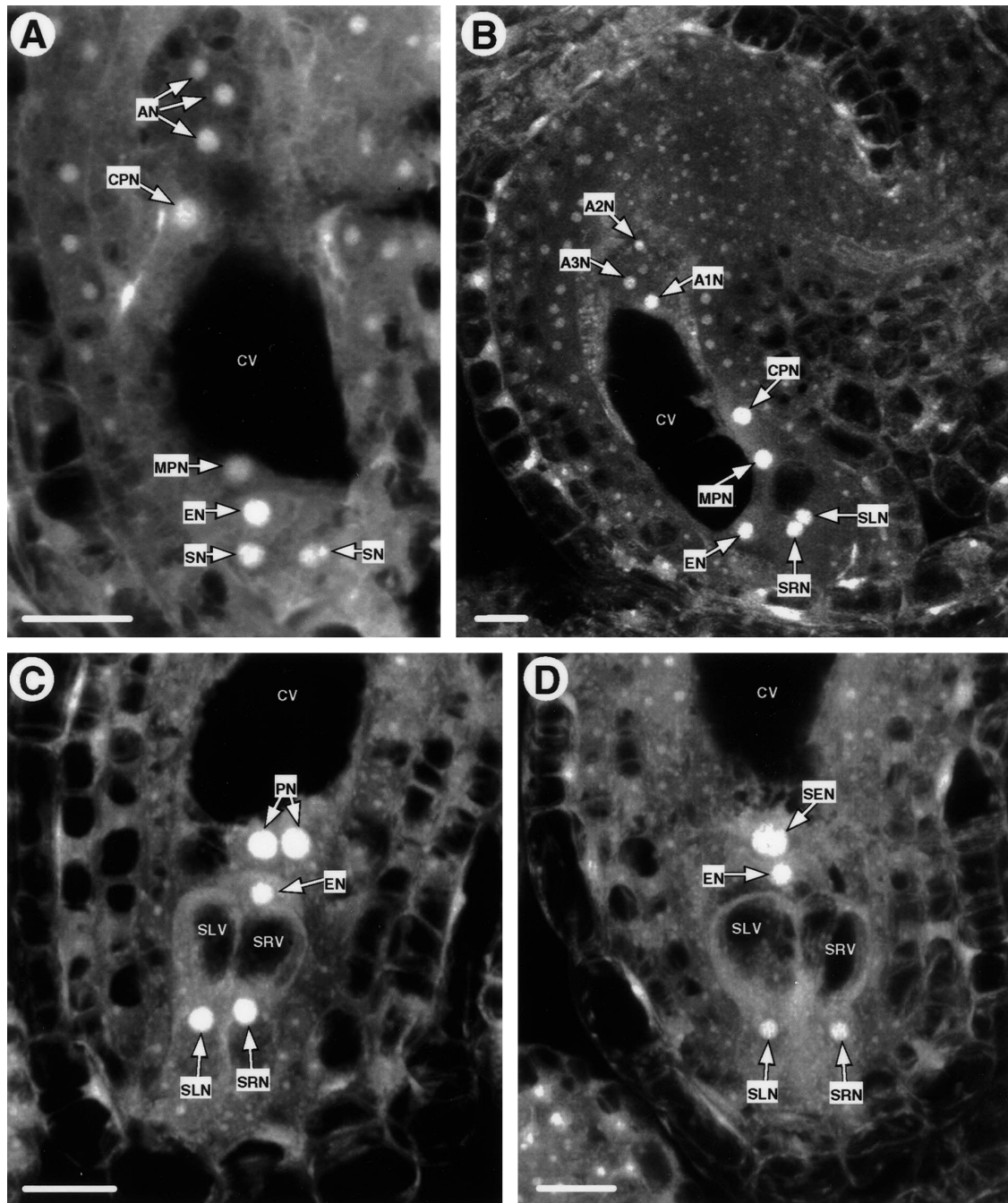
The degenerate megaspores are still present during stage FG2. We observed stage FG2 much less frequently than stages FG1 and FG3, suggesting that stage FG2 is short-lived and that formation of the central vacuole (discussed below) occurs shortly after mitosis. At stage FG2, the ovule's inner integument is approximately two-thirds the length of the nucellus, and the outer integument surrounds the inner integument and completely encloses the nucellus. This is in contrast to previous studies in which enclosure by the outer integument was reported to occur at a later stage (Robinson-Beers et al. 1992; Webb and Bowman 1994).

Late two-nucleate stage (stage FG3)

Stage FG3, shown in Fig. 2D, is defined by the presence of a prominent central vacuole in the two-nucleate fe-

male gametophyte. This vacuole separates the two nuclei to the chalazal and micropylar poles. Toward the end of stage FG3, an additional smaller vacuole forms at the chalazal pole. Throughout this stage, degenerate megaspores are still present. During stage FG3, the female gametophyte first becomes curved as a consequence of the ovule's anatropous orientation. At stage FG3 and subsequent stages, the ovule's inner and outer integuments both completely enclose the nucellus. A two-nucleate female gametophyte with a prominent central vacuole is frequently observed among *Polygonum*-type species (Maheshwari 1950; Willemse and van Went 1984; Haig 1990; Reiser and Fischer 1993).

Four-nucleate stage (stage FG4)

The developing female gametophyte next undergoes a second round of mitosis to produce a four-nucleate female gametophyte, which we define as stage FG4. We were able to identify developing embryo sacs in early and late stage FG4 (see Materials and methods). Figure 3A and Fig. 3B show early and late stage FG4, respectively. During this stage, the chalazal nuclei and the micropylar nuclei are separated by a large central vacuole. A second smaller vacuole is also present at the chalazal pole. Female gametophyte curvature, as a consequence of the ovule's anatropous orientation, is very conspicuous during stage FG4 and all subsequent stages. Degenerate megaspores are no longer apparent at stage FG4 (Fig. 3A).

In a female gametophyte at early stage FG4, the two chalazal nuclei lie along a line that is orthogonal to the chalazal-micropylar axis (Fig. 3A). In a late stage FG4 female gametophyte, by contrast, the two chalazal nuclei lie along a line that is parallel to the chalazal-micropylar axis (Fig. 3B). Thus, during stage FG4, the chalazal nuclei migrate such that the line between them rotates approximately 90° relative to the chalazal-micropylar axis.

In most (>90%) late stage FG4 female gametophytes observed, the micropylar nuclear pair lie along a line that is orthogonal to the chalazal-micropylar axis, as shown in Fig. 3B. Infrequently, however, we also observed late stage FG4 female gametophytes in which the micropylar nuclear pair lie along a line that is parallel to the chalazal-micropylar axis or slightly offset from this (data not shown). These observations suggest that the micropylar nuclei may also migrate to become parallel to the chalazal-micropylar axis. The low frequency of these observations indicates that if micropylar nuclear migration does occur, it probably occurs just prior to the third mitosis. Nuclear migration in the four-nucleate embryo sac has been observed in other *Polygonum*-type species (Folsom and Cass 1990; Huang and Sheridan 1994)

Eight-nucleate stage (stage FG5)

Stage FG5 is the most active stage of female gametophyte development. During this stage, the female gametophyte progresses from an eight-nucleate coenocyte to a seven-celled embryo sac.

Stage FG5 is shown in Figs. 4A–C and 5A–D. Stage FG5 begins as the developing female gametophyte undergoes a third and final round of mitosis. The initial result is an eight-nucleate cell with four nuclei at each pole separated by a central vacuole (Fig. 4A). Two major events occur during stage FG5. The first is a dramatic migration of one nucleus from each pole (the polar nuclei) toward each other and the second is cellularization.

Polar nuclei migration begins immediately after the third mitosis. The chalazal polar nucleus migrates most of the length of the embryo sac along the adaxial surface (Figs. 4B, 5A). The micropylar polar nucleus, by contrast, migrates a much shorter distance along the adaxial surface (Figs. 4B, 5B). As a consequence, the polar nuclei meet in the embryo sac's micropylar half, at a position that is toward the adaxial surface and very close to the egg nucleus (Fig. 4C). Just prior to fusion, the nucleoli of the two polar nuclei lie adjacent to each other, forming an axis almost perpendicular to the chalazal-micropylar axis (Fig. 4C) (Mansfield et al. 1991).

Cellularization is completed during stage FG5. Figures 4C and 6A show that during late stage FG5 the female gametophyte cells have conspicuous cell boundaries, vacuoles, and distinct polarities. During early stage FG5, cell boundaries can also be seen, but the cells have neither well-developed vacuoles nor distinct polarities (data not shown). Taken together, these data indicate that cellularization begins early during stage FG5, probably immediately after the third mitosis (Schneitz et al. 1995), and is completed before polar nuclei fusion.

Figure 5 contains serial optical sections of a developing female gametophyte at mid stage FG5 (the projection of these optical sections is shown in Fig. 4B). This figure shows that by this time the female gametophyte cells occupy specific positions and have distinct polarities. At the micropylar end, the two synergid cells lie along the adaxial surface (Figs. 1A, 5A, D) and the egg cell lies along the abaxial surface (Figs. 1A, 5C). When viewed from the abaxial direction (Fig. 1B), the two synergid cells lie side by side, defining a "left synergid" and a "right synergid" (Figs. 1B, 4C). At the chalazal end are the three antipodal cells (Figs. 1A, 4B, 5B–D). The center of the embryo sac is occupied by the very large central cell with its two unfused polar nuclei (Figs. 4B, C, and 5A, B). This cellular arrangement is consistent with prior studies in *Arabidopsis* (Mansfield et al. 1991; Murgia et al. 1993; Schneitz et al. 1995) and is typical of *Polygonum*-type embryo sacs (Maheshwari 1950; Willemse and van Went 1984). By mid stage FG5, the egg, synergid, and central cells have become highly vacuolate (Fig. 5). The positioning of these vacuoles gives the cells a distinct polarity (discussed below), indicating that these cells have developed unique cell identities.

Seven-celled stage (stage FG6)

Stage FG6 is shown in Fig. 4D. Stage FG6 begins as the two polar nuclei fuse. Polar nuclei fusion occurs toward the adaxial surface of the embryo sac and at a position that is about one-fourth the female gametophyte's length
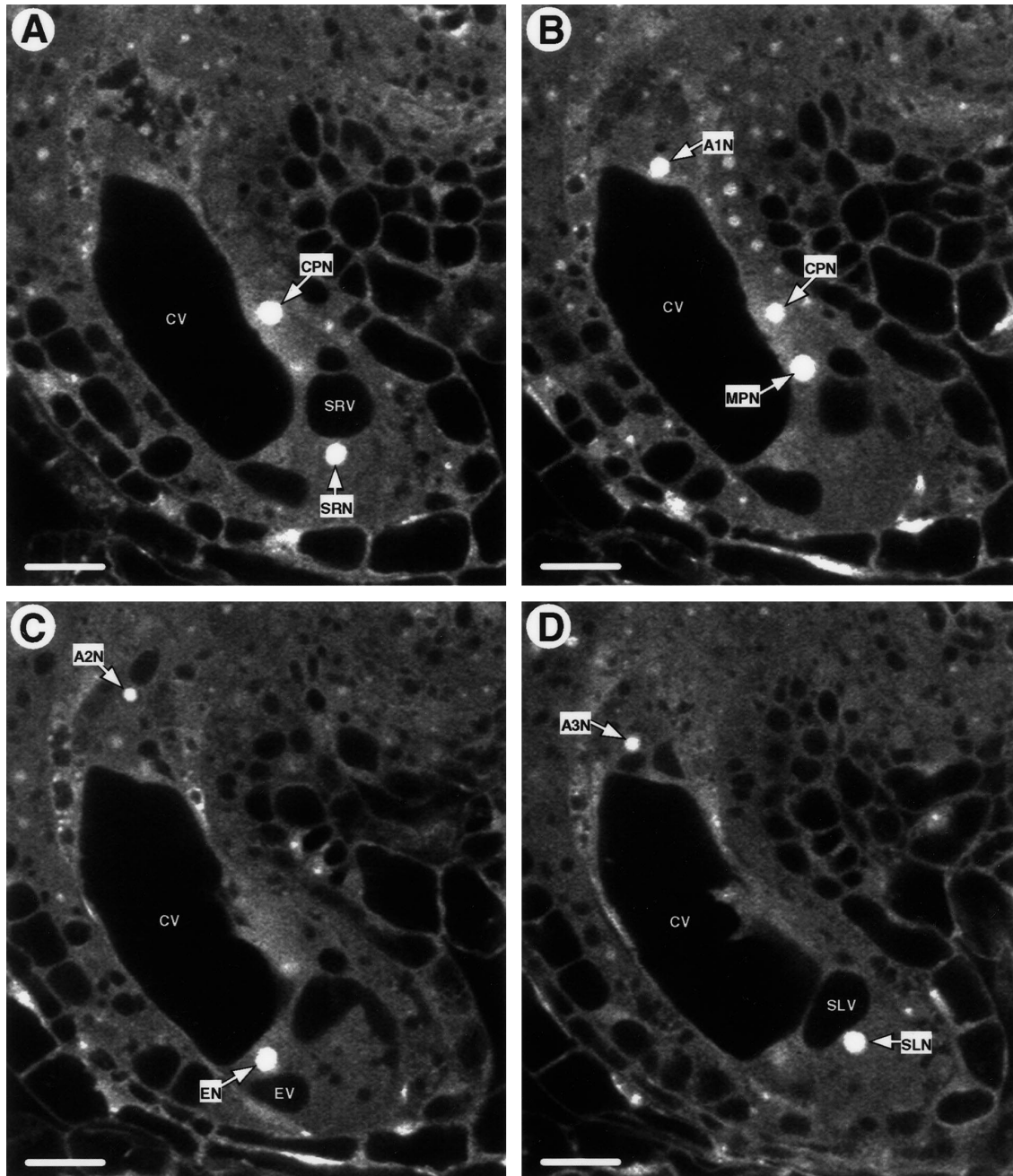
Fig. 5A–D Serial optical sections of a mid stage FG5 female gametophyte. Each image consists of a single 1.5 µm optical section. The image in Fig. 4B is a projection of the four sections shown in this figure *A1N, A2N, A3N, SLN* and *SRN* correspond to the nuclei of the same names in Fig. 4B. **A** Serial optical section number 1 showing the "right" synergid cell (nucleus, *SRN* and vacuole, *SRV*) and the chalazal polar nucleus (*CPN*). **B** Serial optical section number 2 showing one of the antipodal cells (*A1N*), the chalazal polar nucleus (*CPN*), and the micropylar polar nucleus (MPN). **C** Serial optical section number 3 showing one of the antipodal cells (*A2N*) and the egg cell (nucleus, *EN* and vacuole, *EV*). **D** Serial optical section number 4 showing one of the antipodal cells (*A3N*) and the "left" synergid cell (nucleus, *SLN* and vacuole, *SLV*). In all panels, the female gametophyte is oriented with the adaxial surface to the right, the abaxial surface to the left, the micropylar pole down, and the chalazal pole up. *CV* central cell vacuoles. *Bars*=10 µm

from the micropylar pole. The diploid nucleus created by polar nuclei fusion is called the secondary endosperm nucleus and is the nucleus of the central cell.

During stage FG6, the antipodal cells lose their prominence and eventually disappear. We consistently observed degeneration of the three antipodal cells (Poliakova 1964; Murgia et al. 1993; Schneitz et al. 1995). Antipodal cell degeneration is shown in Fig. 6A–C. During late stage FG5, the antipodal cells are at their maximum prominence (Fig. 6A). During stage FG6, the antipodal cell cluster becomes increasingly compact and less distinguishable from the surrounding chalazal nucellus (Fig. 6B). Eventually, the antipodal cells are no longer
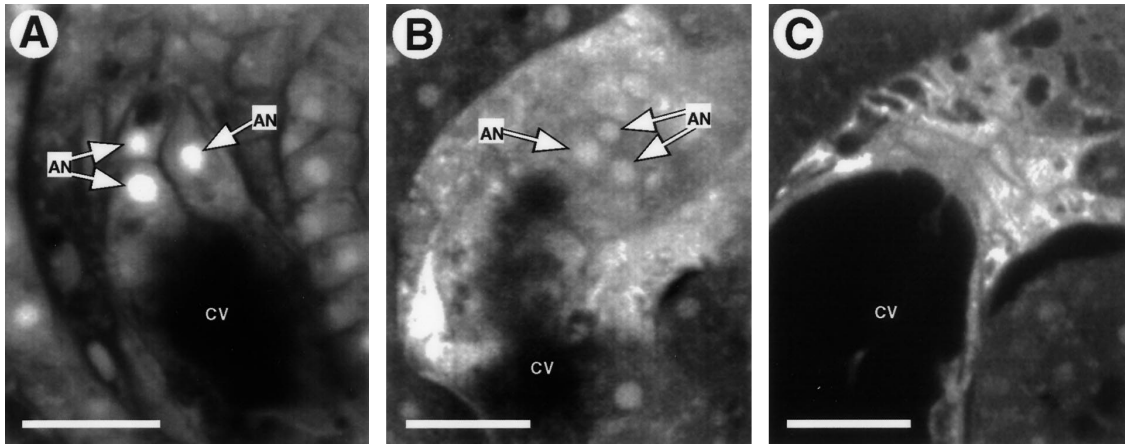
Fig. 6A–C Antipodal cell degeneration. **A** CLSM image of the chalazal pole at late stage FG5. The antipodal cells are at their maximum prominence. This image is a projection of three 1.5 μm optical sections. **B** CLSM image of the chalazal pole at mid stage FG6. The antipodal cells are in the process of degeneration and are not distinguishable from the surrounding chalazal nucellus. This image is a projection of three 1.5 μm optical sections. **C** CLSM image of the chalazal pole at stage FG7. The antipodal cells are absent. This image consists of a single 1.5 μm optical section. In all panels, the female gametophytes are oriented with the adaxial surface to the right, the abaxial surface to the left, the micropylar pole down, and the chalazal pole up. *AN* Antipodal nuclei, *CV* central cell vacuole. Bars=10 μm

distinguishable and the tissue at the chalazal nucellus is highly autofluorescent under 568 nm excitation (Fig. 6C).

Our analysis clearly indicates that at the time of polar nuclei fusion the antipodal cells are still prominent and, thus, that antipodal cell degeneration occurs after polar nuclei fusion. This observation is in contrast to those by Poliakova (1964), who reported that antipodal degeneration occurs before polar nuclei fusion. Murgia et al. (1993) and Schneitz et al. (1995) did not relate the timing of polar nuclei fusion to that of antipodal degeneration.

Four-celled stage (stage FG7)

Stage FG7 is shown in Fig. 7A, 7B. The complete disappearance of the antipodal cells defines the beginning of stage FG7. Thus, during this stage, the female gametophyte consists of the four cells (central cell, egg cell, and two synergid cells) that constitute the female germ unit (Dumas et al. 1984).

Figure 7A is a longitudinal section of a stage FG7 female gametophyte at the micropylar pole. This figure shows a synergid cell lying along the adaxial surface and the egg cell lying along the abaxial surface. The second synergid cell also lies along the adaxial surface, but in a different plane of section. The extreme micropylar portion of the embryo sac is occupied by the two synergid cells (Fig. 7A), causing the egg cell to occupy a more chalazal position. Because the egg and synergid cells are

about the same length (egg, 19.4±0.6 μm, *n*=10; synergids, 21.1±1.1 μm, *n*=20), the egg cell's chalazal tip extends above (more chalazal) the synergid cells' chalazal tips (Fig. 7A, B). This cellular arrangement is consistent with prior studies in *Arabidopsis* (Mansfield et al. 1991; Murgia et al. 1993) and is typical of *Polygonum*-type embryo sacs (Willemse and van Went 1984).

Figure 7A shows that the egg, synergid, and central cells are highly polarized (Mansfield et al. 1991; Murgia et al. 1993; Schneitz et al. 1995). The egg cell's nucleus and most of its cytoplasm are present at its chalazal pole and a large vacuole occupies the micropylar two-thirds of the cell (Figs.1A, B and 7A). Egg cell polarization is almost universal among the angiosperms (Maheshwari 1950; Willemse and van Went 1984; Russell 1993) and might be involved in establishing apical-basal polarity during embryogenesis (Natesh and Rau 1983; West and Harada 1993). The synergid cells have the opposite polarity of the egg cell, with their nuclei positioned at their micropylar poles and their vacuoles at their chalazal poles (Figures 1A, 1B, and 7A). The central cell is likewise polarized, with its nucleus and an accumulation of cytoplasm adjacent to the egg apparatus (Figs. 1A, B and 7A). As a result, the secondary endosperm nucleus and the egg nucleus lie very close to each other. Figure 7B is a transmission electron micrograph showing that the nuclei of these two cells lie within 1.2 μm of each other, presumably to facilitate double fertilization. Figure 7A, B shows the relative size of the egg, synergid, and central cell nucleoli. The egg cell's nucleolus is slightly larger than that of the synergid cell (Fig. 7A). However, the central cell's nucleolus is dramatically larger than that of the other two cells (Fig. 7A, B). The *Arabidopsis* female germ unit's cellular morphology is typical of that found among the angiosperms (Maheshwari 1950; Willemse and van Went 1984; Russell 1993).

Three-celled stage (stage FG8)

Stage FG8, shown in Fig. 7C, is marked by the degeneration of one synergid cell. We found that synergid cell de-
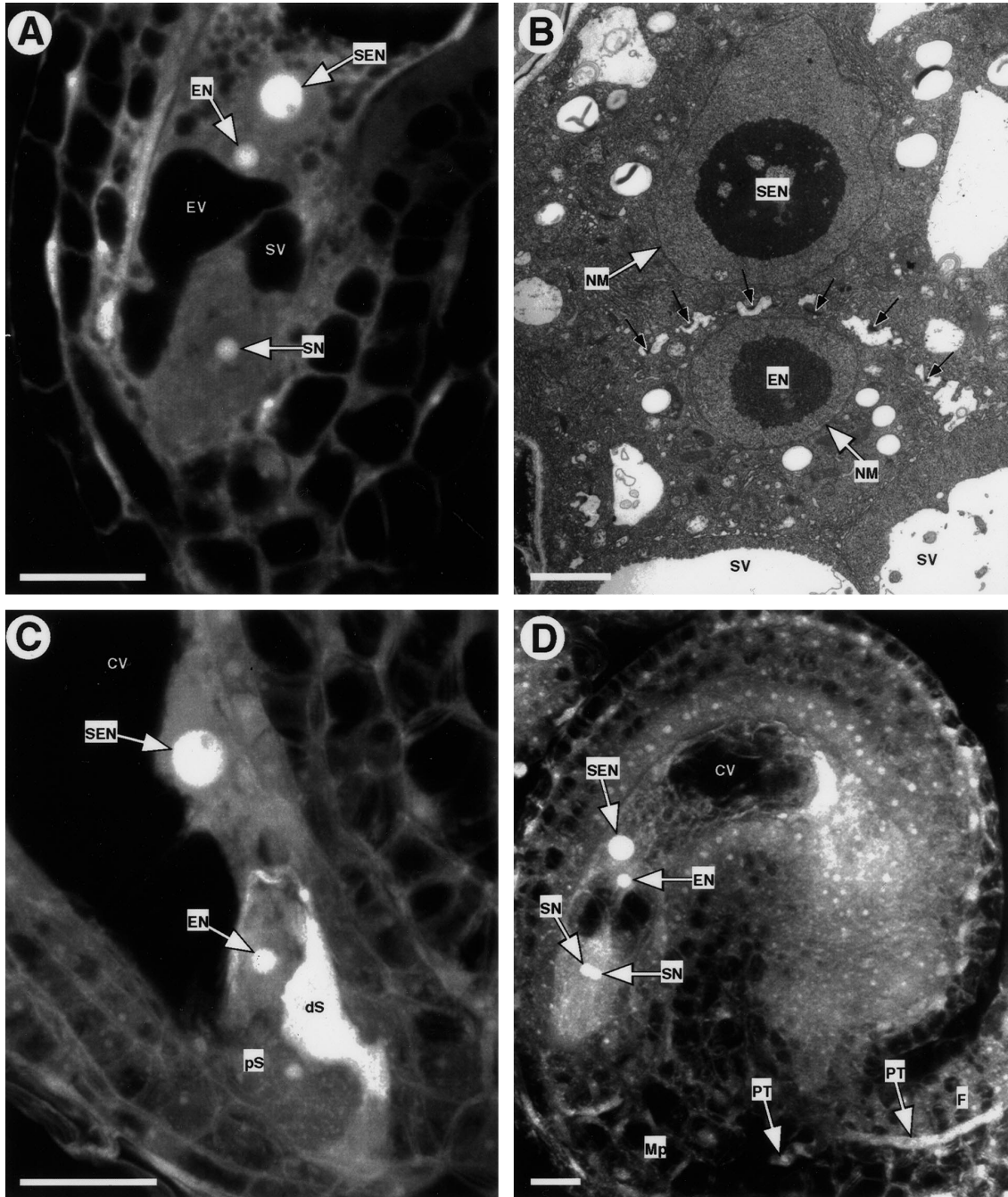
Fig. 7A–D Stages FG7 and FG8 of *Arabidopsis* female gameto-phyte development. **A** CLSM image of the micropylar region of a stage FG7 female gametophyte. This panel shows a synergid cell (nucleus, *SN* and vacuole, *SV*) lying along the adaxial surface and the egg cell (nucleus, *EN* and vacuole, *EV*) lying along the abaxial surface. The synergid cell shown is the right synergid (Fig. 1B). This image consists of a single 1.5 μm optical section. *Bar*=10 μm. **B** Transmission electron micrograph of the nuclei in the egg and central cells from a stage FG6 female gametophyte. The nuclear membranes (*NM*) lie very close to each other (approximately 1.2 μm). The darker-staining region within each nucleus is the nucleolus. The *black arrows* indicate regions of cell wall deposition between the egg and central cells. *Bar*=3 μm. **C** CLSM image of a developing female gametophyte at stage FG8. The female gametophyte consists of three cells: one central cell (secondary endosperm nucleus, *SEN* and vacuole, *CV*), one egg cell (*EN*), and one persistent synergid cell (*pS*). One of the synergid cells (*dS*) degenerates. This image is a projection of three 1.5 μm optical sections. *Bar*=10 μm. **D** CLSM image of a female gametophyte just prior to fertilization. This image shows a pollen tube (*PT*) on the funiculus (*F*) and tracking toward the micropyle (*Mp*). In this female gametophyte both synergid cells (*SN*) are intact. This image is a projection of nine 1.5 μm optical sections. *Bar*=10 μm. The female gametophytes in **A C** and **D** are oriented with their adaxial surface to the right, their abaxial surface to the left, their micropylar pole down, and their chalazal pole up. The female gametophyte in **B** is viewed from the abaxial surface and oriented with its micropylar pole down, and its chalazal pole up

generation occurs consistently, and well after antipodal cell degeneration (Murgia et al. 1993). Using CLSM analysis, a degenerating synergid cell exhibits three morphological features: (1) strong whole-cell autofluorescence, (2) absence of a vacuole, and (3) lack of a distinguishable nucleolus. An FG8 female gametophyte therefore consists of only three cells: one central cell, one egg cell, and one synergid cell.

To determine whether a specific synergid cell degenerates, we identified stage FG8 female gametophytes and determined whether it was the left or right synergid cell (defined in Fig. 1B) that degenerated. Of 11 stage FG8 female gametophytes observed, six had a degenerating left synergid and five had a degenerating right synergid. Thus, within the context of the female gametophyte, the selection of which synergid cell undergoes degeneration appears to be a random process.

Table 4 Synchrony of female gametophyte development in L-*er*

Pistil number	Number of female gametophytes at developmental stages							
	FG0	FG1	FG2	FG3	FG4	FG5	FG6	FG7
1	18	2						
2	10	13						
3	1	19						
4		14	4	2				
5			2	15	3			
6				6	15			
7				1	19	1		
8					2	12		
9						9	1	
10						12	8	
11						9	1	3
12						4	2	8
13						1	3	7
14						1	1	10
15							3	10

Synergid cell degeneration occurs as a consequence of pollination

In *Arabidopsis*, flower development stage 14 (Smyth et al. 1990) begins as the long stamens extend above the stigma and self-pollination occurs. Table 3 shows that the late stages of female gametophyte development [stages FG6 (seven-celled stage) to FG8 (three-celled stage)] occur during flower development stage 14. Thus, at the time of pollination, female gametophyte development is not yet complete. This raised the possibility that pollination might trigger some late events of female gametophyte development such as polar nuclei fusion, antipodal degeneration, or synergid degeneration. To address this issue, we analyzed female gametophyte development in the absence of pollination. We emasculated flowers at flower development stage 12c (defined in Materials and methods), waited 24–72 h, and fixed pistils for CLSM analysis. In a parallel experiment, we hand-pollinated emasculated flowers at 24 h following emasculation. With unpollinated flowers, all of the events occurring up to and including stage FG7 (four-celled stage) occurred normally. However, the primary event of stage FG8 (three-celled stage), synergid cell degeneration, was never observed in over 100 ovules examined. With the pollinated flowers, by contrast, we consistently observed female gametophytes either with a degenerating synergid cell or with only one remaining synergid cell. Taken together, these data indicate that synergid cell degeneration occurs as a consequence of pollination.

In all species examined (except those lacking synergid cells), the pollen tube enters the female gametophyte by penetrating one of the synergid cells, and it is the penetrated synergid cell that degenerates. In some species, synergid cell degeneration occurs prior to pollen tube arrival, but, in other species, this process occurs after pollen tube arrival (van Went and Willemse 1984; Willemse and van Went 1984; Russell 1993). To determine whether synergid cell degeneration occurs before or after pollen tube arrival in *Arabidopsis*, we analyzed synergid

cell morphology in ovules just prior to pollen tube arrival. We identified 14 ovules in which the pollen tube was on the ovule. Of these, two ovules had a pollen tube on the funiculus, nine ovules had a pollen tube in the micropyle, and three ovules had a pollen tube adjacent to and touching a synergid cell. In all such ovules observed, both synergid cells were intact and showed no signs of degeneration; that is, they were not autofluorescent and had distinguishable vacuoles and nucleoli. For example, Fig. 7D shows an ovule with a pollen tube on the funiculus and with both synergid cells intact. These data suggest very strongly that in *Arabidopsis*, synergid cell degeneration occurs after pollen tube arrival.

Synchrony of female gametophyte development

To determine the extent to which female gametophyte development within a pistil is synchronous, we fixed pistils from L-*er* flowers at a variety of developmental stages and scored the developmental stages of the female gametophytes within these pistils using CLSM. The results of this analysis are given in Table 4 and reveal two important points. First, within all pistils, only a narrow range of developmental stages was present. Generally, the range was two developmental stages. The exceptions were those pistils containing female gametophytes at stages FG2 (early two-nucleate stage) or FG6 (seven-celled stage), most likely because these two stages are short lived (discussed above). Second, within most pistils, one developmental stage predominated. Generally, >75% of the female gametophytes within a pistil were at that developmental stage. Some pistils contained approximately equal numbers of female gametophytes at two developmental stages (e.g., pistil numbers 2 and 10) and thus were considered to be at the transition between those two stages. Taken together, these data indicate that female gametophyte development within a pistil is fairly synchronous and that, within a range, it is possible to as-

Table 5 Summary of CLSM analysis of the *Gf* mutant

Developmental stage analyzed[a]	Number of pistils analyzed	Number of normal FGs observed	Number of abnormal FGs observed
FG1 (One-nucleate)	4	45	0
FG3/4 (Late two-nucleate/four-nucleate)	1	12	8
FG4 (Four-nucleate)	2	20	11
FG4/5 (Four-nucleate/eight-nucleate)	2	10	9
FG5/6 (Eight-nucleate/seven-celled)	3	25	23
FG7 (Four-celled)	12	90	80

[a] Assignment of a female gametophyte stage to a pistil is described in Materials and methods

Fig. 8 Morphology of *Gf* female gametophytes. CLSM image of an abnormal female gametophyte from a *Gf/GF* pistil at stage FG7. This image shows a female gametophyte (*mFG*) arrested at the uninucleate stage. This image is a single 1.5 μm optical section. *mFG* Mutant female gametophyte, *N* nucleus. *Bar*=10 μm

sign a female gametophyte developmental stage to a pistil (see Materials and methods).

Phenotypic analysis of the *Gf* mutant

The *Gf* mutation was originally identified by Redei in the 1960s (Redei 1965). Genetic analysis showed that *Gf* affects both the female and the male gametophytes, is fully penetrant in the female gametophyte, and is partially penetrant in the male gametophyte (Redei 1965). From the analysis of paraffin-sectioned material, it was reported that *Gf* female gametophytes appeared morphologically normal except for a low frequency of twin embryo sacs (Redei 1965).

We analyzed development of *Gf* female gametophytes throughout megagametogenesis using CLSM. To determine the terminal phenotype of *Gf* female gametophytes, we emasculated *Gf/GF* flowers at flower development stage 12c (defined in Materials and methods), waited 48 h, fixed the pistils for CLSM analysis, and analyzed 170 female gametophytes. When this was done with wild-type pistils, all female gametophytes observed were at the terminal developmental stage [stage FG7 (four-celled stage)]. In *Gf/GF* pistils, approximately half of the female gametophytes are genotypically mutant (*Gf*) and about half are genotypically wild type (*GF*). As shown in Table 5 (stage FG7 row), approximately half of the female gametophytes were morphologically abnormal, suggesting very strongly that morphologically abnormal female gametophytes were genotypically mutant. Figure 8 shows that abnormal female gametophytes contained one nucleus. In contrast to wild-type female gametophytes at stage FG1 (one-nucleate stage), *Gf* female gametophytes at stage FG7 were not teardrop-shaped, were more expanded, and contained one or more prominent vacuoles (compare Figs. 2B and 8). We observed no twin embryo sacs.

These data suggest that *Gf* female gametophytes fail to progress out of stage FG1 (one-nucleate stage). To verify this, we analyzed female gametophytes at earlier developmental stages. Because female gametophyte de-
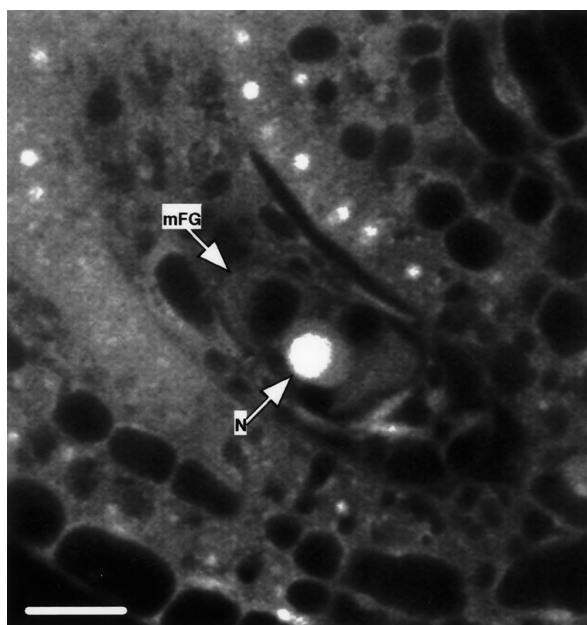
velopment within a pistil is fairly synchronous (Table 4), the wild-type female gametophytes were used to predict the stage of the mutant female gametophytes (discussed in Materials and methods). As shown in Table 5, in *Gf/GF* pistils containing female gametophytes at stages FG3 (late two-nucleate stage) to FG6 (seven-celled stage), approximately half of the female gametophytes analyzed were abnormal. In all cases observed, abnormal female gametophytes displayed the phenotype shown in Fig. 8. By contrast, in pistils containing female gametophytes predominately at stage FG1 (one-nucleate stage), all embryo sacs observed were indistinguishable from wild type. [Pistils containing female gametophytes predominantly at stage FG2 (early two-nucleate stage) were not analyzed because, as shown in Table 4, they would contain significant numbers of female gametophytes at stage FG1 (one-nucleate stage).] Taken together, these data indicate that the *Gf* mutation affects female gametophyte development and that mutant female gametophytes fail to progress out of stage FG1 (one-nucleate stage).

Discussion

Megagametogenesis in *Arabidopsis* wild type

We analyzed *Arabidopsis* megagametogenesis using CLSM. Our results are in general agreement with those of previous studies (Misra 1962; Poliakova 1964; Webb and Gunning 1990; Mansfield et al. 1991; Murgia et al.

1993; Webb and Gunning 1994; Schneitz et al. 1995). However, the advantages of CLSM have allowed us to extend these prior studies and to make several new observations.

Sequence of events

We have unambiguously determined that the following events occur in a specific sequence: (1) first mitosis, (2) central vacuole formation, (3) second mitosis, (4) third mitosis, (5) cellularization, (6) polar nuclei fusion, (7) antipodal degeneration, and (8) synergid degeneration. Based on this sequence of events, we divided *Arabidopsis* female gametophyte development into eight stages (Table 1). We developed this staging system primarily to provide a framework for mutant analysis and have already used it in our analysis of the *Gf* mutant. However, it also will be an essential tool for describing gene expression patterns during female gametophyte development. Our female gametophyte staging system complements the staging systems for *Arabidopsis* flower development (Smyth et al. 1990) and *Arabidopsis* ovule development (Schneitz et al. 1995).

Synchrony

We found that female gametophyte development within a pistil is fairly synchronous (Table 4). Thus, within a range, it is possible to assign a female gametophyte stage to a pistil (see Materials and methods). This feature is extremely useful for mutant analysis because in the pistils of a plant heterozygous for a female gametophyte mutation, the developmental stage of the wild-type female gametophytes can be used to determine the approximate developmental stage of the genotypically mutant and morphologically abnormal female gametophytes present in the same pistil (Table 5). For example, in our analysis of the *Gf* mutant, we were able to determine that the genotypically mutant and morphologically abnormal female gametophyte in Fig. 8 was at stage FG7 (four-celled stage).

Nuclear migration in the four-nucleate embryo sac

We found that during stage FG4 (four-nucleate stage), the chalazal nuclear pair initially lie orthogonal to the chalazal-micropylar axis (Fig. 3A), but that they migrate such that they become parallel to the chalazal-micropylar axis (Fig. 3B). We also found that the micropylar nuclear pair may migrate to occupy a position parallel to the chalazal-micropylar axis. Nuclear migration in a four-nucleate embryo sac has been observed in several other species (Folsom and Cass 1990; Russell 1993; Huang and Sheridan 1994). In such cases, the micropylar-most nucleus of the chalazal pair gives rise to one polar nucleus and one antipodal nucleus, and the chalazal-most nucleus

of the chalazal pair gives rise to two antipodal nuclei (Brown 1909; Cooper 1937; Folsom and Cass 1990; Huang and Sheridan 1994). Likewise, the chalazal-most nucleus of the micropylar pair divides to form the egg and micropylar polar nuclei, and the micropylar-most nucleus of the micropylar pair gives rise to the two synergid nuclei (Schaffner 1901; Brown 1909; Brown and Sharp 1911; Ishikawa 1918; Howe 1926; Johanhsen 1929; Cooper 1937; Palser et al. 1971; Howe 1975; Folsom and Cass 1990; Russell 1993; Huang and Sheridan 1994). Thus, the nuclear migrations we observed in *Arabidopsis* probably have determinative consequences.

Synergid cell degeneration

We found that if pollination is inhibited, synergid cell degeneration does not occur in *Arabidopsis*. Thus, although synergid cell degeneration is a component of the flower developmental program, it is not an intrinsic step of the female gametophyte developmental program. These data indicate that the terminal developmental stage in *Arabidopsis* is stage FG7 (four-celled stage) and that the mature embryo sac consists of one central cell, one egg cell, and two synergid cells. These four cells constitute the female germ unit, which is the minimum cell complement required for reproduction (Dumas et al. 1984; Russell 1993). Whether synergid cell degeneration is an intrinsic step of the female gametophyte developmental program in other species is not well studied. However, in cotton, synergid cell degeneration occurs in cultured ovules that are unpollinated and unfertilized (Jensen et al. 1977). Thus, in at least one species, synergid cell degeneration appears to be an intrinsic step of the female gametophyte developmental program.

Our data show that synergid cell degeneration is triggered by pollination in *Arabidopsis*. The signal to trigger synergid cell degeneration may be either long-range (diffusible) or require cell-cell contact. We found that synergid cell degeneration occurs after pollen tube arrival, suggesting that degeneration is triggered by pollen tube contact in *Arabidopsis*. In several other species, including *Capsella*, the synergid does not degenerate until pollen tube arrival (Schulz and Jensen 1968; van Went 1970; Newcomb 1973). However, in most species examined, synergid cell degeneration occurs prior to pollen tube arrival (Jensen 1965; Diboll 1968; Cocucci and Jensen 1969; Cass and Jensen 1970; Chao 1971; Maze and Lin 1975; Mogensen and Suthar 1979; Wilms 1981). Synergid cell degeneration prior to pollen tube arrival suggests the existence of a long-range signal; however, in these species, it has not been determined whether pollination is required for degeneration. In at least one species, pollination is not required for synergid cell degeneration (Jensen et al. 1977).

We observed that either synergid cell can degenerate. Thus, within the developmental context of the female gametophyte, synergid degeneration appears to be a random event. However, Murgia et al. (1993) reported that

the synergid cell that degenerates is the one that is located on the side that is closest to the placenta. Similar observations have been observed in other species (Mogensen 1984; Yan et al. 1991). Thus, within the developmental context of the carpel, synergid cell degeneration may not be a random event (Murgia et al. 1993).

CLSM analysis of megagametogenesis mutants

From analysis of paraffin-sectioned material, it was previously reported that *Gf* female gametophytes appeared morphologically normal except for a low frequency of twin embryo sacs (Redei 1965). In contrast to these earlier studies, we did not observe twin embryo sacs. Furthermore, we found that the *Gf* mutation has a dramatic effect on female gametophyte development. We found that *Gf* female gametophytes fail to progress beyond stage FG1 (one-nucleate stage). Nevertheless, mutant embryo sacs remain viable, become more expanded and develop one or more prominent vacuoles (Fig. 8). This indicates that the *GF* gene product is not required for cell viability and that rather, it is required for progression out of stage FG1 (one-nucleate stage). The *Gf* mutation exhibits reduced transmission through the male gametophyte (Redei 1965), indicating that the *GF* gene also functions during pollen development. Because the *Gf* mutation is fully penetrant in the female gametophyte, it cannot become homozygous; thus, it cannot be determined whether the *GF* gene functions during sporophyte development.

Several other mutations affecting female gametophyte development or function have been identified, including the *Arabidopsis trp4 trp1* (Niyogi et al. 1993), *ctr1* (Kieber et al. 1993), *emb173* (Castle et al. 1993), and *prl* (Springer et al. 1995) mutations, as well as the maize *ig* (Kermicle 1971), *lo1* (Singleton and Mangelsdorf 1940), *lo2* (Nelson and Clary 1952), and *sp* (Singleton and Mangelsdorf 1940) mutations. Of these, morphological analysis throughout megagametogenesis has been carried out only with the *ig* mutant (Lin 1978, 1981; Huang and Sheridan 1996). The *ig* mutation appears to affect primarily regulation of the nuclear division cycle resulting in asynchronous and/or extra nuclear divisions, and causing multiple secondary defects, including abnormal microtubule patterns, abnormal nuclear migration, abnormal nuclear positioning, and lack of cellular specialization of micropylar cells.

We recently developed a genetic screen for female gametophyte mutants, and have identified over 20 mutants with defects in megagametogenesis or female gametophyte function (C.A. Christensen, S. Subramanian, and G.N. Drews, unpublished). Our preliminary data suggest that the frequency of female gametophyte mutations is extremely high (C.A. Christensen, S. Subramanian, and G.N. Drews, unpublished). Thus, a procedure to rapidly determine the phenotype of a female gametophyte mutant is required. In this paper, we demonstrate that our CLSM procedure is effective for rapidly analyzing hundreds of developing female gametophytes to determine the phenotype of a megagametophyte mutant. For example, approximately 1 day was required to perform the *Gf* mutant characterization presented here. We are currently using this procedure in conjunction with our genetic screen to identify female gametophyte mutants with defects in specific cellular and developmental processes such as the establishment of female gametophyte polarity, specification of female gametophyte cell identity, mitosis, central vacuole formation, cell expansion, nuclear migration, polar nuclei fusion, cellularization, programmed cell death, pollen tube-female gametophyte interaction, fertilization, and the induction of seed development.

References

Bouman F (1984) The ovule. In: Johri BM (ed) Embryology of angiosperms. Springer, Berlin Heidelberg New York, pp 123–157

Brown WH (1909) The embryo sac of *Habenaria*. Bot Gaz 48: 241–250

Brown WH, Sharp LW (1911) The embryo sac of *Epipactis*. Bot Gaz 52:439–452

Cass DD, Jensen WA (1970) Fertilization in barley. Am J Bot 57:62–70

Castle LA, Errampalli D, Atherton TL, Franzmann LH, Yoon ES, Meinke DW (1993) Genetic and molecular characterization of embryonic mutants identified following seed transformation in *Arabidopsis*. Mol Gen Genet 241:504–514

Chao C-Y (1971) A periodic acid-Schiff's substance related to the directional growth of pollen tube into embryo sac in *Paspalum* ovules. Am J Bot 58:649–654

Cocucci A, Jensen WA (1969) Orchid embryology: megagametophyte of *Epidendrum scutella* following fertilization. Am J Bot 56:629–640

Cooper DC (1937) Macrosporogenesis and embryo-sac development in *Euchlaena mexicana* and *Zea mays*. J Agric Res (Washington DC) 55:539–551

Diboll A (1968) Fine structural development of the megagametophyte of *Zea mays* following fertilization. Am J Bot 55:787–806

Dumas C, Knox RB, McConchie CA, Russell SD (1984) Emerging physiological concepts in fertilization. What's New Plant Physiol 15:17–20

Folsom MW, Cass DD (1990) Embryo sac development in soybean: cellularization and egg apparatus expansion. Can J Bot 68:2135–2147

Haig D (1990) New perspectives on the angiosperm female gametophyte. Bot Rev 56:236–275

Howe TD (1926) Development of embryo sac in *Grindelia squarrosa*. Bot Gaz 81:280–296

Howe TD (1975) The female gametophyte of three species of *Grindelia* and of *Prionopsis ciliata* (Compositae). Am J Bot 62:273–279

Huang B-Q, Sheridan WF (1994) Female gametophyte development in maize: microtubular organization and embryo sac polarity. Plant Cell 6:845–861

Huang B-Q, Sheridan WF (1996) Embryo sac development in the maize indeterminate gametophyte1 mutant: abnormal nuclear

behavior and defective microtubule organization. Plant Cell 8:1391–1407

Hulskamp M, Schneitz K, Pruitt RE (1995) Genetic evidence for a long-range activity that directs pollen tube guidance in *Arabidopsis*. Plant Cell 7:57–64

Ishikawa RM (1918) Studies on the embryo sac and fertilization of *Oenothera*. Ann Bot (London) 32:279–317

Jensen WA (1965) The ultrastructure and histochemistry of the synergids of cotton. Am J Bot 52:238–256

Jensen WA, Schulz P, Ashton ME (1977) An ultrastructural study of early endosperm development and synergid changes in unfertilized cotton ovules. Planta 133:179–189

Johanhsen DA (1929) Studies on the morphology of Onograceae. I. The megagametophyte of *Hartmannia tetraptera*. Bull Torrey Bot Club 56:285–299

Kermicle JL (1969) Androgenesis conditioned by a mutation in maize. Science 166:1422–1424

Kermicle JL (1971) Pleiotropic effects on seed development of the indeterminate gametophyte gene in maize. Am J Bot 58:1–7

Kieber JJ, Rothenberg M, Roman G, Feldman KA, Ecker JR (1993) *CTR1*, a negative regulator of the ethylene response pathway in *Arabidopsis*, encodes a member of the Raf family of protein kinases. Cell 72:427–441

Kobayashi M, Tsunewaki K (1980) Haploid induction and its genetic mechanism in alloplasmic common wheat. J Hered 71:9–14

Koltunow AM (1993) Apomixis: embryo sacs and embryos formed without meiosis or fertilization in ovules. Plant Cell 5:1425–1437

Lin B-Y (1978) Structural modifications of the female gametophyte associated with the *indeterminate gametophyte* (*ig*) mutant in maize. Can J Genet Cytol 20:249–257

Lin B-Y (1981) Megagametogenetic alterations associated with the indeterminate gametophyte (*ig*) mutation in maize. Rev Brasil Biol 41:557–563

Maheshwari P (1950) An introduction to the embryology of angiosperms. McGraw-Hill, New York

Mansfield SG, Briarty LG, Erni S (1991) Early embryogenesis in *Arabidopsis thaliana*. I. The mature embryo sac. Can J Bot 69:447–460

Maze J, Lin S-C (1975) A study of the mature megagametophyte of *Stipa elmeri*. Can J Bot 53:2958–2977

Misra RC (1962) Contribution to the embryology of *Arabidopsis thaliana* (Gay and Monn.). Agra Univ J Res Sci 11:191–199

Modrusan Z, Reiser L, Feldman KA, Fischer RL, Haughn GW (1994) Homeotic transformation of ovules into carpel-like structures in *Arabidopsis*. Plant Cell 6:333–349

Mogensen HL (1984) Quantitative observations on the pattern of synergid degeneration in barley. Am J Bot 71:1448–1451

Mogensen HL, Suthar HK (1979) Ultrastructure of the egg apparatus of *Nicotiana tabacum* (Solanaceae) before and after fertilization. Bot Gaz 140:168–179

Murgia M, Huang B-Q, Tucker SC, Musgrave ME (1993) Embryo sac lacking antipodal cells in *Arabidopsis thaliana* (Brassicaceae). Am J Bot 80:824–838

Natesh S, Rau MA (1983) The embryo. In: Johri BM (ed) Embryology of angiosperms. Springer, Berlin Heidelberg New York, pp 377–443

Nelson OE, Clary GB (1952) Genetic control of semi-sterility in maize. J Hered 43:205–210

Newcomb W (1973) The development of the embryo sac of sunflower *Helianthus annuus* before fertilization. Can J Bot 51:863–878

Niyogi KK, Last RL, Fink GR, Keith B (1993) Suppressors of *trp1* fluorescence identify a new *Arabidopsis* gene, *TRP4*, en-

coding the anthranilate synthase beta subunit. Plant Cell 5:1011–1027

Nogler GA (1984) Gametophytic apomixis. In: Johri BM (ed) Embryology of angiosperms. Springer, Berlin Heidelberg New York, pp 159–196

Ohad N, Margossian L, Hsu Y-C, Williams C, Repetti P, Fischer RL (1996) A mutation that allows endosperm development without fertilization. Proc Natl Acad Sci USA 93:5319–5324

Palser BF, Philipson WR, Philipson MN (1971) Embryology of *Rhododendron*. J Indian Bot Soc 50:172–188

Poliakova TF (1964) Development of the male and female gametophytes of *Arabidopsis thaliana* (L) Heynh. Issled Genet 2:125–133

Redei GP (1965) Non-mendelian megagametogenesis in *Arabidopsis*. Genetics 51:857–872

Reiser L, Fischer RL (1993) The ovule and the embryo sac. Plant 5:1291–1301

Robinson-Beers K, Pruitt RE, Gasser CS (1992) Ovule development in wild-type *Arabidopsis* and two female sterile mutants. Plant Cell 4:1237–1249

Russell SD (1993) The egg cell: development and role in fertilization and early embryogenesis. Plant Cell 5:1349–1359

Schaffner JH (1901) A contribution to the life history and cytology of *Erythronium*. Bot Gaz 31:369–378

Schneitz K, Hulskamp M, Pruitt RE (1995) Wild-type ovule development in *Arabidopsis thaliana*: a light microscope study of cleared whole-mount tissue. Plant J 7:731–749

Schulz R, Jensen WA (1968) *Capsella* embryogenesis: the synergids before and after fertilization. Am J Bot 55:541–552

Singleton WR, Mangelsdorf PC (1940) Gametic lethals on the fourth chromosome of maize. Genetics 25:366–389

Smyth DR, Bowman JL, Meyerowitz EM (1990) Early flower development in *Arabidopsis*. Plant Cell 2:755–767

Springer PS, McCombie WR, Sundaresan V, Martienssen RA (1995) Gene trap tagging of *PROLIFERA*, an essential *MCM2-3–5*-like gene in *Arabidopsis*. Science 268:877–880

Tsunewaki K, Mukai Y (1990) Wheat haploids through the Salmon method. In: Bajaj YPS (ed) Wheat. (Biotechnology in agriculture and forestry, vol 13). Springer, Berlin Heidelberg New York, pp 460–478

Webb MC, Bowman JL (1994) Stages of embryo sac and ovule development. In: Bowman JL (ed) *Arabidopsis*: an atlas of morphology and development. Springer, Berlin Heidelberg New York, p 300

Webb MC, Gunning BES (1990) Embryo sac development in *Arabidopsis thaliana*. I. Megasporogenesis, including the microtubular cytoskeleton. Sex Plant Reprod 3:244–256

Webb MC, Gunning BES (1994) Embryo sac development in *Arabidopsis* thaliana. II. The cytoskeleton during megagametogenesis. Sex Plant Reprod 7: 153–163

Went JL van (1970) The ultrastructure of the synergids of *Petunia*. Acta Bot Neerl 19:121–127

Went JL van, Willemse MTM (1984) Fertilization. In: Johri BM (ed) Embryology of angiosperms. Springer, Berlin Heidelberg New York, pp 273–317

West MAL, Harada JJ (1993) Embryogenesis in higher plants: an overview. Plant Cell 5:1361–1369

Willemse MTM, Went JL van (1984) The female gametophyte. In: Johri BM (ed) Embryology of angiosperms. Springer, Berlin Heidelberg New York, pp 159–196

Wilms HJ (1981) Pollen tube penetration and fertilization in spinach. Acta Bot Neerl 30:101–122

Yan H, Yang HY, Jensen WA (1991) Ultrastructure of the developing embryo sac of sunflower (*Helianthus annuus*) before and after fertilization. Can J Bot 69:191–202